result does not parallel a previous observation on similar rhenium(V) dioxo complexes with acyclic tetraamines exhibiting *two* IR bands at 810 and 790 cm^{-1} attributed to the stretching vibrations of the same group.[6] The complex cation *trans*-$[ReO_2(cyclam)]^+$ (**4**) shows both types of absorptions assigned to the *trans*-$[ReO_2]^+$ group depending on the particular counterion in the salts **4**(ReO_4), **4**(Cl), and **4**(PF_6). The complexes **4**(ReO_4) and **4**(Cl) have *one* band at 772 cm^{-1}, and **4**(PF_6) has *two* bands at 809 and 776 cm^{-1}. Previously, it has been reported that the salt $[ReO_2(cyclam)Cl\cdot 2[B(C_6H_5)_3\cdot H_2O]$ [**4**(BPh_3)] exhibits *one* absorption at 825 cm^{-1}.[16] The presence of a *single* or *double* absorption in complexes containing the *trans*-MO_2 arrangement is not uncommon, and a similar behavior has been observed for *trans*-OsO_2^{2+} and *trans*-UO_2^{2+} complexes.[20] This behavior has been generically attributed to unit-cell coupling.[6,21] However, the X-ray crystallographic analysis of **4**(PF_6) shows that the complex cation $[ReO_2(cyclam)]^+$ lies on an inversion center (Figure 2). Since the site group does not alter the inversion symmetry of the free cation, it seems unlikely that the doubling of the $[ReO_2]^+$ stretch in **4**(PF_6) originates from unit-cell splitting. Considering that the unit cell of **4**(PF_6) includes two molecules of the complex cation which are not related by any symmetry operation of the space group, we suggest assignment of the two observed absorptions to the *single* asymmetric stretching of the $[ReO_2]^+$ group associated with each one of the two inequivalent sets of molecules. This interpretation is consistent with the finding that the unit cell of **4**(BPh_3), which shows *one* IR absorption, includes two symmetry-equivalent molecules of cation **4**.[16] The observed differences in the values of the *trans*-dioxo asymmetric stretching frequencies between the species **4**(Cl), **4**(BPh_3), and the two independent complex cations in **4**(PF_6) may be probably ascribed to van der Waals interactions of the different crystalline environments. Similar effects have been already observed, and Bandoli et al. reported a definite example of the change of the IR stretching frequencies upon variation of the crystalline form for the technetium(III) complex $Tc(pd)_2(PPh_3)Cl$ (pd = pentane-2,4-dionato).[22]

Acknowledgment. S.A.L. is grateful to the Italian Ministero degli Esteri for a grant at the University of Ferrara. We thank M. Fratta for elemental analyses, L. Zuppiroli for mass spectral measurements, and A. Aguiari for scanning electron microprobe analysis. This work was supported by the Ministero dell'Università e della Ricerca Scientifica e Tecnologica.

Registry No. **1**, 25685-08-9; **2**, 16853-54-6; **3**, 34387-57-0; **4**(ReO_4), 141040-25-7; **4**(Cl)$_n$, 117579-37-0; **4**(PF_6), 141040-26-8; *trans*-$[ReO_2(L')]Cl$, 140874-56-2; *trans*-$[ReO_2(L')]PF_6$, 140874-58-4; *trans*-$[ReO_2(en)_2]Cl$, 14405-69-7; *trans*-$[ReO_2(pn)_2]Cl$, 93192-00-8.

Supplementary Material Available: Tables of all refined atomic coordinates (Table A), anisotropic thermal parameters (Table B), and complete bond distances and angles (Table C) and ORTEP diagrams of the conformation of the cyclam ligand (Figure 3) and of the possible network of intermolecular hydrogen bondings (Figure 4) in $[ReO_2(cyclam)](PF_6)$ (6 pages); a listing of observed and calculated structure factors (18 pages). Ordering information is given on any current masthead page.

(20) (a) McGlynn, S. P.; Smith, J. K.; Neely, W. C. *J. Chem. Phys.* **1961**, *35*, 105-116. (b) Bullock, J. I. *J. Chem. Soc. A* **1969**, 781-784.
(21) Hornig, D. F. *J. Chem. Phys.* **1948**, *16*, 1063-1076.
(22) (a) Bandoli, G.; Clemente, D. A.; Mazzi, U. *J. Chem. Soc., Dalton Trans.* **1977**, 1837-1844. (b) Bandoli, G.; Clemente, D. A.; Mazzi, U.; Roncari, E. *Acta Crystallogr., Sect. B: Struct. Crystallogr. Cryst. Chem.* **1978**, *B34*, 3359-3361.

Contribution from the Departamento de Química, Instituto de Ciências e Engenharia Nucleares-Laboratório Nacional de Engenharia e Tecnologia Industrial, P-2686 Sacavém Codex, Portugal, and Centro de Química Estrutural, Instituto Superior Técnico, P-1096 Lisboa Codex, Portugal

Low-Dimensional Molecular Metals $(Per)_2M(mnt)_2$ (M = Fe and Co)

Vasco Gama,[†] Rui T. Henriques,[†] Grégoire Bonfait,[†] Laura C. Pereira,[†] João C. Waerenborgh,[†] Isabel C. Santos,[†] M. Teresa Duarte,[‡] João M. P. Cabral,[†] and Manuel Almeida*[,†]

Received July 13, 1991

Single crystals of the quasi-one-dimensional conductors $(Per)_2M(mnt)_2$, M = Fe and Co (Per = perylene, mnt = maleonitriledithiolate), were prepared by electrocrystallization. By X-ray diffraction at room temperature and with synchrotron radiation (λ = 0.89 Å, at Daresbury), the $(Per)_2Fe(mnt)_2$ compound was shown to crystallize in the monoclinic space group $C2/c$ with cell parameters a = 50.571 (6) Å, b = 8.212 (2) Å, c = 17.726 (9) Å, β = 92.43 (1)°, and Z = 8. An average crystal structure was obtained at 295 K using a conventional X-ray source, on the basis of the monoclinic space group $P2_1/n$ with a = 17.665 (3) Å, b = 4.098 (2) Å, c = 25.219 (3) Å, β = 92.43 (2)°, and Z = 2. The average crystal structure of $(Per)_2Fe(mnt)_2$ at room temperature consists of a close-packed arrangement of segregated stacks of perylene and $Fe(mnt)_2$ units. ^{57}Fe Mössbauer spectroscopy shows the dimerization of the $Fe(mnt)_2$ units with the Fe atom in a square pyramidal coordination by sulfur atoms without significant changes within the temperature range 15-295 K. For both compounds, room temperature values of electrical conductivity and absolute thermoelectric power are $\sigma_{RT} \simeq 200\ \Omega^{-1}\ cm^{-1}$ and $S_{RT} = 42\ \mu V/K$, respectively. They exhibit metallic behavior down to 58 and 73 K, for M = Fe and Co, respectively, where a metal-insulator transition occurs. The paramagnetic susceptibility of the Co compound is due to a Pauli-like contribution of the perylene chains of 3.2×10^{-4} emu mol^{-1} at 300 K that vanishes at the metal-insulator transition, while that of the Fe compound is dominated by the contribution of antiferromagnetically coupled pairs of $S = {}^3/_2$ spins in the $[Fe(mnt)_2]_2^{2-}$ units, in a way similar to the magnetic susceptibility of $[(C_2H_5)_4N]_2[Fe(mnt)_2]_2$ and $[(n\text{-}C_4H_9)_4N]_2[Fe(mnt)_2]_2$. These properties and the average crystal structure are compared with the correspondent ones for other metallic members of the $Per_2M(mnt)_2$ family.

Introduction

Several molecular metals based on perylene (Per (I)) and on square planar anionic metal complexes ($M(mnt)_2$ (II), where mnt = maleonitriledithiolate or *cis*-2,3-dimercapto-2-butenedinitrile) with the general formula $(Per)_2M(mnt)_2$, where M = Pt, Pd, Au, Cu, and Ni, have been studied in the last years.[1-6]

[†] Laboratório Nacional de Engenharia e Tecnologia Industrial.
[‡] Instituto Superior Técnico.

(1) Alcácer, L.; Novais, H.; Pedroso, F.; Flandrois, S.; Coulon, C.; Chasseau, D.; Gaultier, J. *Solid State Commun.* **1980**, *35*, 945.
(2) Henriques, R. T.; Alcácer, L.; Pouget, J. P.; Jérome, D. *J. Phys. C: Solid State Phys.* **1984**, *17*, 5197.

0020-1669/92/1331-2598$03.00/0

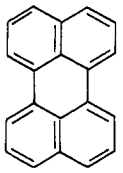

I

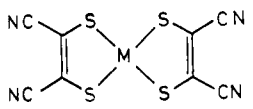

II

Some members of this family (e.g., M = Pt, Pd) have spin exchange between the conduction electrons in stacks of perylene molecules and the localized magnetic momenta in stacks of $M(mnt)_2$.[4] At low temperatures they undergo metal–insulator transitions associated with a lattice dimerization[2] and a decrease of the magnetic susceptibility. Due to the simultaneous presence of conducting and magnetic chains in the crystal structure, the mutual interaction between the chains, each one a priori with Peierls or spin-Peierls instabilities, offers a wide range of possible theoretical situations to be considered for the explanation of the observed phase transitions, making this family of compounds unique and very interesting among low-dimensional systems.

In order to get further information concerning the nature of the metal–insulator transition in these compounds and the role of the organometallic counterions and their magnetic moment, we decided to explore new compounds of this family containing organometallic counterions already with chemically induced dimerization at room temperature, either diamagnetic or paramagnetic. For this purpose we selected the species $M(mnt)_2^-$, M = Fe and Co, which, as opposed to the cases studied before, are known to exist as dimers with the metal close to the sulfur atom of a neighbor $M(mnt)_2$ unit, in a five-coordination configuration.[7,8] In this paper we report the synthesis and physical characterization of $Per_2M(mnt)_2$, M = Fe and Co, single crystals prepared by electrocrystallization. Preliminary data on the transport properties of these compounds were recently reported.[9]

Experimental Section

Synthesis and Electrocrystallization. $(Per)_2[M(mnt)_2]$, M = Fe and Co, single crystals were prepared by electrochemical oxidation of perylene in a dichloromethane solution ($\simeq 10^{-2}$ M) containing $(n\text{-}C_4H_9)_4N[Fe(mnt)_2]$ in stoichiometric proportion by a procedure identical to those previously described for other compounds of this family.[1,6] Special care was taken with the previous purification of the starting reagents. Perylene (Sigma) was gradient sublimed (10^{-2} Torr, 110 °C) several times after pentane recrystallization and alumina–silica chromatography,[10] and $(n\text{-}C_4H_9)_4N[Fe(mnt)_2]$ and $(n\text{-}C_4H_9)_4N[Co(mnt)_2]$, prepared as previously described,[11-13] were recrystallized from acetone–diethyl ether for M = Co and from acetone–isobutanol for M = Fe. Dichloromethane (Merck Uvasol) was dried with molecular sieves and passed through an alumina column just before use, and the solutions were deaerated with argon. The electrocrystallization was performed in a two-compartment cell on platinum electrodes through a galvanostatic technique,[14] using current densities in the range 2–10 $\mu A/cm^2$. For M = Fe, black needle-shaped crystals with metallic shine, often with fibrous appearance and typical dimensions up to $\simeq 15 \times 1.0 \times 0.10$ mm^3, were collected from the anode compartment after $\simeq 5$ days and washed with dichloromethane.

Table I. Crystal Data and Structure Analysis Results for $(Per)_2Fe(mnt)_2$

chemical formula	$FeN_4S_4C_{48}H_{24}$
formula weight	840.85
crystal system	monoclinic
space group	$P2_1/n$
a, Å	17.665 (3)
b, Å	4.098 (2)
c, Å	25.219 (2)
β, deg	92.43 (2)
V, Å^3	1824 (2)
Z	2
D_{calc}, g/cm^3	1.531
$F(000)$, electrons	860
μ(Mo Kα), cm^{-1}	56.5
temperature, K	295
2θ range, deg	3–120
no. of total data	2521
no. of unique data	2232
observed data ($I \geq 1.5\sigma(I)$)	1303
final agreement factor R^a	0.111
largest peak in final Fourier difference map, e/Å^3	1.9

$^a R = \sum(||F_o| - |F_c||)/\sum F_o$.

Elemental analysis using a Perkin-Elmer 240 elemental analyzer at the analytical service of our laboratory gave the following results. Found: C, 68.54; H, 2.73; N, 6.50. Anal. Calcd for $FeS_4N_4C_{48}H_{24}$: C, 68.56; H, 2.88; N, 6.66.

For M = Co, the crystals obtained by the same procedure were also black and with metallic shine, but in many preparations most of them (>95%) were thick ($\simeq 3 \times 0.2 \times 0.2$ mm^3) with a distinct habit, with only a minor amount of thinner and distinct needle-shaped crystals ($\simeq 5 \times 0.05 \times 0.02$ mm^3). The thick crystals correspond to a different stoichiometry (Per $Co(mnt)_2(CH_2Cl_2)_{0.5}$) as reported elsewhere,[15] and in this paper we will refer only to the thin crystals that, as will become clear by analogy of the physical properties with the Fe compound and with elemental analysis, correspond to $(Per)_2Co(mnt)_2$. Exceptionally, one batch was obtained with mainly these thin and long needle-shaped crystals, which were selected for magnetic susceptibility and elemental analysis with the following results. Found: C, 67.85; H, 2.38; N, 6.64. Anal. Calcd for $CoS_4N_4C_{28}H_{24}$: C, 68.31; H, 2.87; N, 6.64.

X-ray Crystallography. Weissenberg photographic techniques showed for both compounds (with M = Fe and Co) weak reflections in layers of odd k corresponding to a doubling of the cell along b with $b \simeq 8$ Å. These reflections were not intense enough to be measured by the standard automatic techniques. So M = Fe crystals were analyzed at the Synchroton radiation source (SERC—Daresbury Laboratory). Data was conclusive, showing that the crystal belonged to monoclinic space group $C2/c$ with $a = 50.571$ (6) Å, $b = 8.212$ (2) Å, $c = 17.726$ (9) Å, $\beta = 92.43$ (1)°, and $Z = 8$. However, the poor quality of the crystals, the reflections defining the lattice doubling being relatively weak and not very well defined, together with significant crystal decay during the radiation exposure percluded structure solution with the synchrotron data. Therefore, the structure reported here is an average structure obtained by using data collected on a Rigaku AFC5R automatic diffractometer with graphite-monochromated Cu Kα radiation ($\lambda = 1.541\,78$ Å) from a 12-kW rotating anode generator, in a ω–2θ scan mode (Molecular Structure Corp.). A black, plate-shaped crystal of $(Per)_2Fe(mnt)_2$ having dimensions of $0.36 \times 0.04 \times 0.005$ mm^3 was measured at room temperature. Unit cell dimensions were obtained by least-squares refinement of the setting angles of 25 automatically centered reflections with $7.1° < \theta < 30°$. Three standard reflections were monitored during data collection, and no decay or instrumental instability was detected. Data was corrected for Lorentz and polarization but not for absorption effects. The structure was solved by the Patterson method using SHELX76.[16] All non-hydrogen atoms were sucessively located from difference Fourier synthesis. Full-matrix least-squares refinement was used with all non-hydrogen atoms, refining anisotropically. Hydrogen atoms were inserted in idealized positions and allowed to refine with an overall atomic displacement parameter. Final refinement converged to $R = 0.112$. A final electron density of 2.02 electrons/Å^3 was obtained near the Fe atom ($x = 0.0009$, $y = 0.1326$, $z = 0.1860$). Crystallographic details are listed in Table I. Scattering factors were taken from ref 17. All calculations

(3) Henriques, R. T.; Almeida, M.; Matos, M. J.; Alcácer, L.; Bourbonnais, C. *Synth. Met.* **1987**, *19*, 379.
(4) Alcácer, L. *Mol. Cryst. Liq. Cryst.* **1985**, *120*, 221.
(5) Domingos, A.; Henriques, R. T.; Gama, V. P.; Almeida, M.; Lopes Vieira, A.; Alcácer, L. *Synth. Met.* **1989**, *27*, B411.
(6) Gama, V. P.; Almeida, M.; Henriques, R. T.; Santos, I. C.; Domingos, A.; Ravy, S.; Pouget, J. P. *J. Phys. Chem.* **1991**, *95*, 4263.
(7) Hamilton, W. C.; Bernal, I. *Inorg. Chem.* **1967**, *6*, 2003.
(8) Balch, A. L.; Dance, I. G.; Holm, R. H. *J. Am. Chem. Soc.* **1968**, *90*, 1139.
(9) Gama, V. P.; Henriques, R. T.; Almeida, M. In *Lower Dimensional Solids and Molecular Devices*, Metzger, R. M., Day, P., Papavassiliou, G., Eds.; NATO-ASI; Plenum Press: 1991; p 222.
(10) Raymond, J.; Sangster, C.; Irvine, J. W., Jr. *J. Chem. Phys.* **1956**, *24*, 670.
(11) Eaton, G. R.; Holm, R. H. *Inorg. Chem.* **1971**, *10*, 805.
(12) Weiher, J. F.; Melby, L. R.; Benson, R. E. *J. Am. Chem. Soc.* **1964**, *86*, 4329.
(13) Davison, A.; Holm, H. R. *Inorg. Synth.* **1967**, *10*, 8.
(14) Engler, E. M.; Greene, R.; Haen, P.; Tomkiewicz, Y.; Mortensen, K.; Berendzen, J. *Mol. Cryst. Liq. Cryst.* **1982**, *79*, 15.
(15) Gama, V.; Bonfait, G.; Henriques, R. T.; Almeida, M.; Meetsma, A.; van Smaalen, S.; de Boer, J. L. *J. Am. Chem. Soc.* **1992**, *114*, 1986.
(16) Sheldrick, G. M. *SHELX Crystallographic Calculation Program*, University of Cambridge, Cambridge, UK, 1976.

Table II. Fractional Atomic Coordinates ($\times 10^4$ Å) and Equivalent Isotropic Thermal Parameters (Å^2) for $(Per)_2Fe(mnt)_2$

	x	y	z	B_{eq}[a]
Fe(1)	0	0	0	17.3 (4)
S(1)	−1143 (2)	−296 (13)	−364 (2)	5.2 (1)
S(2)	−340 (2)	−3112 (16)	661 (2)	6.7 (2)
C(01)	−1641 (8)	−2334 (38)	96 (5)	3.7 (4)
C(02)	−1305 (8)	−3539 (41)	543 (5)	4.0 (4)
C(03)	−1701 (10)	−5336 (43)	942 (6)	4.9 (5)
C(04)	−2434 (11)	−2729 (51)	−8 (6)	5.4 (6)
N(1)	−1980 (9)	−6942 (44)	1252 (6)	7.4 (6)
N(2)	−3081 (9)	−3066 (48)	−83 (6)	7.1 (6)
C(1)	99 (8)	−10760 (36)	3632 (5)	3.3 (5)
C(2)	49 (9)	−11631 (45)	4152 (6)	4.9 (5)
C(3)	−552 (10)	−13490 (46)	4329 (7)	5.2 (6)
C(4)	−1104 (9)	−14570 (46)	3964 (7)	5.3 (6)
C(5)	−1067 (9)	−13810 (44)	3422 (6)	4.4 (5)
C(6)	−1621 (9)	−15013 (40)	3057 (7)	4.3 (5)
C(7)	−1594 (9)	−14232 (44)	2531 (7)	4.9 (6)
C(8)	−1014 (9)	−12244 (38)	2356 (6)	4.2 (5)
C(9)	−449 (8)	−11028 (38)	2707 (6)	3.7 (5)
C(10)	−464 (8)	−11827 (42)	3253 (6)	3.9 (5)
C(11)	164 (8)	−9032 (44)	2527 (5)	4.0 (5)
C(12)	733 (8)	−7788 (41)	2905 (6)	3.9 (4)
C(13)	715 (8)	−8821 (38)	3438 (5)	3.5 (5)
C(14)	1291 (9)	−7600 (45)	3792 (6)	5.0 (6)
C(15)	1891 (9)	−5769 (42)	3619 (7)	5.1 (6)
C(16)	1908 (9)	−4754 (43)	3096 (7)	5.0 (5)
C(17)	1332 (9)	−6010 (39)	2721 (6)	3.9 (5)
C(18)	1355 (9)	−5033 (42)	2180 (6)	4.7 (5)
C(19)	805 (9)	−6134 (45)	1819 (6)	5.0 (6)
C(20)	223 (9)	−8134 (39)	1996 (6)	4.2 (5)

[a] $B_{eq} = 8\pi^2(^1/_3(U_{11} + U_{22} + U_{33} + 2\cos\beta U_{13})$.

were carried out on a VAX 900 at Instituto Superior Técnico, using SHELX76,[16] PARST,[18] (calculation of geometric data) and PLUTO[19] (illustrations).

Crystals of the Co compound were of poorer diffracting quality than those of Fe, and in this case, Weissenberg photographic techniques using Cu Kα radiation enabled only the confirmation of the space group and the determination of the unit cell parameters indicated in Table III.

Mössbauer Spectroscopy. Mössbauer absorbers ($\simeq$8 mg of Fe/cm^2) were prepared by stacking needle-shaped single crystals of $(Per)_2Fe(mnt)_2$ into a Perspex holder. Mössbauer spectra were measured in transmission mode using a source of ^{57}Co in Rh ($\simeq$20 mCi). The velocity wave had a symmetric "saw-tooth" shape, and the spectrometer was calibrated against an Fe foil absorber. Spectra were obtained with the absorbers at 295, 80, and 15 K using a helium flow cryostat. Computer fitting of the data was performed on folded spectra by assuming doublets of Lorentzian line shape using a nonlinear least-squares method.[20]

Electrical Transport Measurements. The electrical conductivity measurements along the *b* axis of the needles were made in the temperature range 20–300 K using an in-line four-probe configuration and a low-frequency (77 Hz) current of 1 μA, the voltage being measured by a lock-in amplifier (EG&G PAR Model 5301). Gold evaporated contacts on the sample were glued to 25-μm gold wires with platinum paint (Demetron 308A). Special care was taken to select samples with a low ($\leq$1%) unnested/nested voltage ratio as defined by Schaffer et al.[21] The measurements were done in a closed-cycle cryostat (ADP Cryogenics Inc., HC-2/DE202), and the temperature was monitored by a Au (0.07 at. % Fe)–Chromel thermocouple placed close to the sample.

The thermopower was measured, along the *b* axis, relative to gold, in the range 20–350 K, by a slow ac technique (10^{-2} Hz) in an apparatus similar to the one described by Chaikin et al.[22] placed inside the same closed-cycle He cryostat. The thermal gradients used were $\leq$1 K, and they were monitored by a Au (0.07 at. % Fe)–Chromel thermocouple. Absolute thermopower was obtained after correction for the small gold absolute thermopower using the data of Huebner.[23]

Magnetic Susceptibility. Magnetic susceptibility measurements were performed in the range 10–300 K using a Faraday system (Oxford Instruments) with a 7-T superconducting magnet in polycrystalline samples ($\simeq$23 and $\simeq$5 mg for the M = Fe and M = Co compounds, respectively) placed in thin-wall Teflon buckets, previously measured. The magnetic fields used were 2 and 5 T, and force was measured with a microbalance (Sartorius S3D-V) applying forward and reverse gradients of 5 T/m. Under these conditions, the magnetization was found to be proportional to the applied magnetic field.

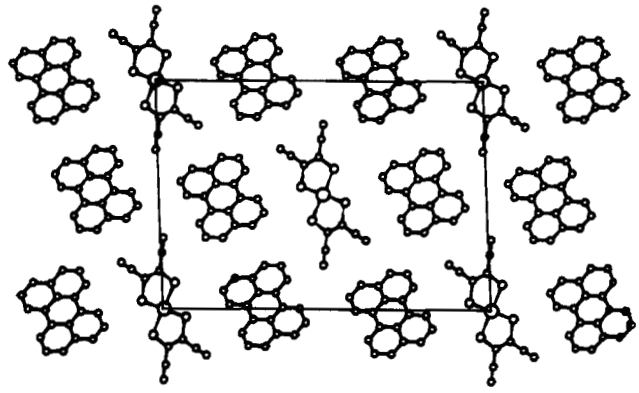

Figure 1. Projection along the *b* axis of the $(Per)_2Fe(mnt)_2$ structure.

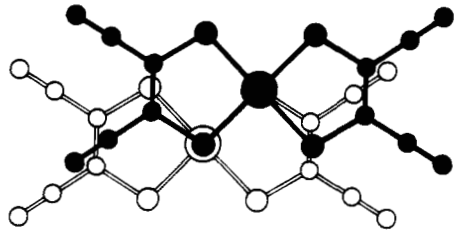

Figure 2. Average overlap mode of $Fe(mnt)_2$ units in $(Per)_2Fe(mnt)_2$.

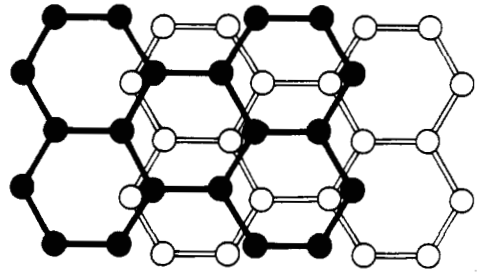

Figure 3. Overlap mode of perylene molecules in $(Per)_2Fe(mnt)_2$.

Results

The $Per_2M(mnt)_2$, M = Fe and Co, compounds have crystal structures different from those of the other metallic members of this series with M = Au,[5] Pd,[5] Pt,[1] Ni,[6] and Cu[6] (see Table III). The difference is visible in the *b* parameter, along the stacking axis, which is doubled as shown by the Weissenberg photographic technique (and Syncroton radiation diffraction for M = Fe) and, in the case of the M = Fe compound, in agreement with the Mössbauer results reported below. The residual electron density observed near the Fe atom is taken also as a possible indication of the dimerization of the $Fe(mnt)_2$ units. The average crystal structure for $(Per)_2Fe(mnt)_2$ obtained in this way clearly shows segregated stacks of perylene and $Fe(mnt)_2$ packed in a way similar to tha analogues with M = Pt,[1] Pd,[5] Au,[5] and Ni.[6] In the unit cell, space group $P2_1/n$, there are four equivalent stacks of perylene molecules and two equivalent stacks of $Fe(mnt)_2$, packed so that each $Fe(mnt)_2$ column is surrounded by six columns of perylene (Figure 1) in the same mode found for other $(Per)_2M(mnt)_2$ compounds.

(17) *International Tables for X-ray Crystallography, Vol. A, Space-Group Symmetry*; Hahn, T., Ed.; Reidel: Dordrecht, The Netherlands, (present distributor Kluwer Academic Publishers, Dordrecht), 1983.
(18) Nardelli, M. *Comput. Chem.* **1983**, *7*, 95.
(19) Motherwell, W. D. S.; Clegg, W. *PLUTO Program for Plotting Molecular and Crystal Structures*; University of Cambridge: Cambridge, England, 1978; unpublished.
(20) Stone, A. J. In Bancroft, G. M.; Maddock, A. G.; Ong, W. K.; Prince, R. H.; Stone, A. J. *J. Chem. Soc. A* **1967**, 1966 (appendix).
(21) Schaffer, P. E.; Wudl, F.; Thomas, G. A.; Ferraris, J. P.; Cowan, D. O. *Solid State Commun.* **1974**, *14*, 347.
(22) Chaikin, P. M.; Kwak, J. F. *Rev. Sci. Instrum.* **1975**, *46*, 218.
(23) Huebner, R. P. *Phys. Rev.* **1964**, *135*, A1281.

Table III. Crystallographic Data on $(Per)_2M(mnt)_2$ α Phases[a]

M	Ni[b]	Cu[b]	Pd[c]	Pt[d]	Au[d]	Fe	Co
a, Å	17.44 (1)	17.6 (1)	16.469 (6)	16.612 (4)	16.602 (2)	50.571 (6)	17.75 (5)
b, Å	4.176 (2)	4.17 (5)	4.1891 (6)	4.1891 (6)	4.194 (1)	8.212 (2)	8.22 (5)
c, Å	25.18 (1)	25.5 (1)	26.640 (9)	26.583 (6)	26.546 (3)	17.726 (4)	25.88 (5)
β, deg	91.57 (2)	91.4 (3)	95.07 (3)	94.54 (2)	94.58 (1)	92.43 (1)	92.0 (3)
V, Å^3	1833 (2)	1856 (10)	1831 (2)	1846 (2)	1841 (1)	7354 (3)	3778 (10)
Z	2	2	2	2	2	8	4

[a] Space group is $P2_1/n$ except for M = Fe, where it is $C2/c$. [b] Reference 6. [c] Reference 1. [d] Reference 5.

Table IV. Mössbauer Data Obtained at Different Temperatures T[a]

absorber	T, K	δ, mm/s	Δ, mm/s	Γ, mm/s	ref
$[Per_2][Fe(mnt)_2]$	295	0.25	2.83	0.26	*b*
	80	0.34	2.79	0.28	*b*
	15	0.36	2.79	0.25	*b*
$[(n\text{-}Bu)_4N]_2[Fe(mnt)_2]_2$	80	0.33	2.68	0.29	*b*
$[(n\text{-}Bu)_4N]_2[Fe(mnt)_2]_2$	295	0.23			25
$[(Et)_4N]_2[Fe(mnt)_2]_2$	295	0.24	2.81		26
	77	0.33	2.76		26

[a] δ, isomer shift relative to metallic iron; Δ, quadrupole splitting; Γ, full width at half-height. Precision in the fitting procedure: ±0.01 mm/s for δ, Δ, and Γ. [b] This work.

In this average structure, the successive $Fe(mnt)_2$ units appear separated by the average distance of 3.46 (3) Å, with the superposition mode shown in Figure 2. When this value is compared to the corresponding one obtained in $[(n\text{-}C_4H_9)_4N]_2[Fe(mnt)_2]_2$, of 2.46 Å,[7] it should be noticed that in this last structure the Fe atom is 0.36 Å out of the best least-squares plane of the four basal sulfur atoms, in a tetrahedically distorted square pyramidal coordination. Due to their inclination angle toward the b axis of 32.4 (3)°, the average distance between consecutive Fe atoms in $(Per)_2Fe(mnt)_2$ is 4.10 (3) Å. In each column of perylene, the distance between successive perylene units is 3.36 (3) Å, with a superposition mode shown in Figure 3. The inclination of the perylene plane toward the b axis is 34.87°.

All Mössbauer spectra were fitted with one quadrupole doublet. For $Per_2Fe(mnt)_2$, both peaks have the same width but different areas (Figure 4); this may be attributed to texture effects as the principal axes of the needle-shaped crystals all lie in a plane perpendicular to the γ-ray direction. This assumption is further confirmed by the observation that the area ratio did not change with temperature and the asymmetry decreased, becoming essentially zero when the angle between the γ rays and the normal of the absorber plane changed from 90° to 54.7°.[24] The estimated parameters are summarized in Table IV together with published values for $[(C_2H_5)_4N]_2[Fe(mnt)_2]_2$[25] and $[(n\text{-}C_4H_9)_4N]_2[Fe(mnt)_2]_2$.[26] Within the experimental error, those parameters are the same for perylene and alkylammonium compounds, the quadrupole splitting, Δ, value for the tetra-*n*-butylammonium compound being slightly lower. The isomer shift, δ, values are compatible with Fe(III) in a square pyramidal configuration. The slight increase in δ as the temperature is lowered is a result of the second-order Doppler effect.

For ethyl- and butylammonium compounds, the anion $Fe(mnt)_2^-$ has been shown to be dimeric as $[Fe(mnt)_2]_2^{2-}$.[7,8] X-ray diffraction in $[(n\text{-}C_4H_9)_4N]_2[Fe(mnt)_2]_2$ showed that each Fe atom is surrounded by five sulfur atoms in a distorted square pyramidal arrangement with an apical Fe–S bond of 2.46 Å.[8] At low temperatures there is no change in the measured δ and Δ values, which is consistent with no significant structural changes in the iron coordination. We therefore can conclude that the Fe environment in the perylene and alkylammonium compounds is the same—dimeric $Fe(mnt)_2$—within the temperature range of 15–295 K. The low half-width, Γ, values, as in the alkylammonium salts, are consistent with only one kind of environment for Fe.

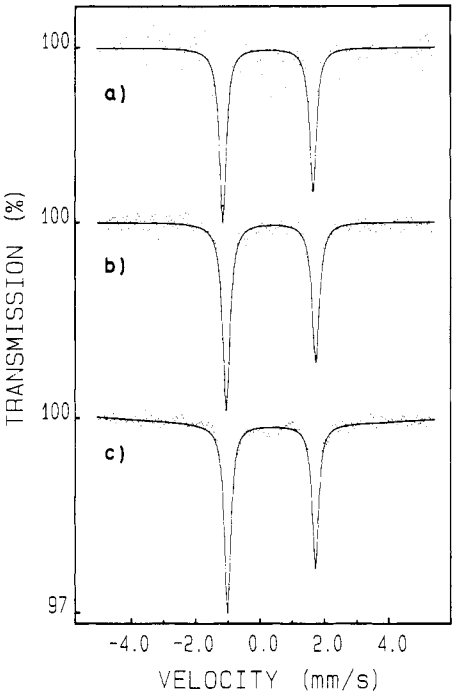

Figure 4. ^{57}Fe Mössbauer spectra of $(Per)_2Fe(mnt)_2$ at 295 (a), 80 (b), and 15 K (c).

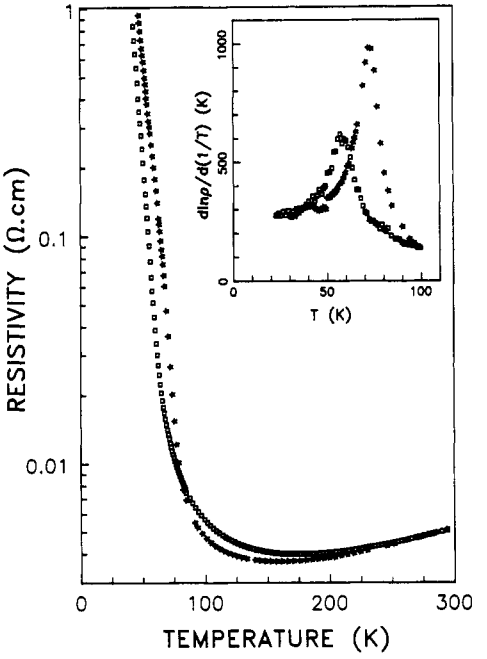

Figure 5. Temperature-dependent resistivity, ρ, along the b axis of $(Per)_2Fe(mnt)_2$ (squares) and $(Per)_2Co(mnt)_2$ (stars). The inset represents d ln ρ/d(1/T) vs T, showing a maximum at 58 K for M = Fe and at 73 K for M = Co.

Electrical conductivity of $(Per)_2M(mnt)_2$ with M = Fe and Co at room temperature is $\simeq$200 Ω^{-1} cm^{-1}. As shown in Figure 5, the electrical resistivity ρ exhibits metallic behavior (dρ/dT >

(24) Ericsson, T.; Wäppling, R. *J. Phys. C6* **1976**, *37*, 719.
(25) Birchall, T.; Greenwood, N. N. *J. Chem. Soc. A* **1969**, 286.
(26) De Vries, J. L. K. F.; Trooster, M.; De Boer, E. *Inorg. Chem.* **1971**, *10*, 81.
(27) Montgomery, H. C. *J. Appl. Phys.* **1971**, *42*, 2971.
(28) Grolemund, V.; Almeida, M., unpublished work.

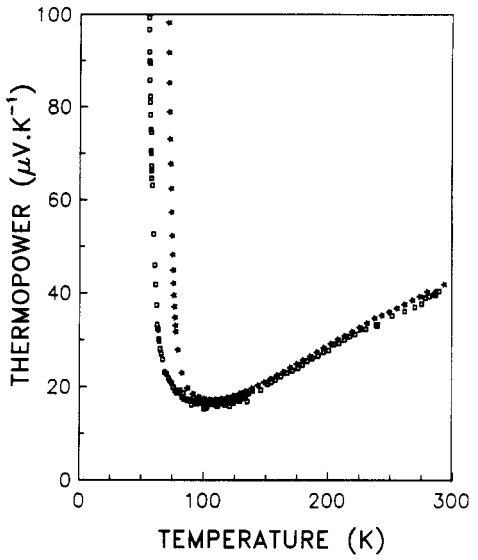

Figure 6. Temperature-dependent absolute thermoelectric power, S, along the b axis of $(Per)_2Fe(mnt)_2$ (squares) and $(Per)_2Co(mnt)_2$ (stars).

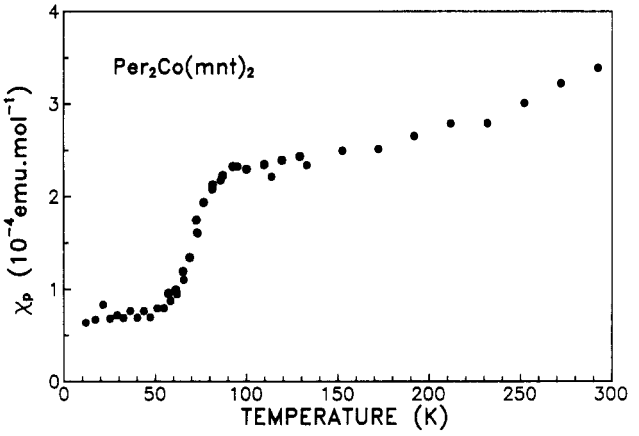

Figure 7. Paramagnetic susceptibility of $(Per)_2Co(mnt)_2$ as a function of temperature T (from experimental values by considering a diamagnetic contribution of 4.2×10^{-4} emu/mol).

0) at high temperature, where ρ is proportional to T^{α} ($\alpha \approx 0.8$–1) and presents a minimum at $T_\rho \simeq 105$ K for M = Fe and at $T_\rho \simeq 95$ K for M = Co. Below T_ρ the electrical resistivity becomes thermally activated, and as shown in Figure 5, there is a metal–insulator (M–I) transition, better seen through the maximum of d ln ρ/d(1/T) at 58 K for M = Fe and at 73 K for M = Co (inset of Figure 5). The resistivity measurements well below T_{M-I} show constant values for d ln ρ/d(1/T), indicative of an energy gap at low temperature of $\simeq$50 and $\simeq$60 meV for the compounds with M = Fe and Co, respectively. The relatively large crystal size of some $(Per)_2Fe(mnt)_2$ samples made it possible to attach well-separated contacts on the opposite sides of platelet crystals (10×1 mm^2) and to measure the anisotropy of the resistivity by the Montgomery technique.[27] These measurements indicate $\rho_\perp/\rho_\parallel = 900$, almost temperature independent down to 100 K.[28]

Room temperature thermopower was found to be $\simeq$42 μV/K for both compounds with M = Co and Fe. In agreement with resistivity data, thermopower measurements in these compounds (Figure 6), with an almost linear dependence on T at high temperatures ($T > 150$ K), are also indicative of metallic behavior. At lower temperature, thermopower varies approximately as $1/T$, a behavior typical of a semiconductor. Thermopower S also shows an anomaly of dS/d(1/T) indicative of a metal–insulator transition but at temperatures slightly below those of the M–I transition temperatures obtained from resistivity data (at 70 K for M = Co and 50 K for M = Fe).

Paramagnetic molar susceptibility, χ_P, of $Per_2Co(mnt)_2$ obtained from magnetization measurements in the range 10–300 K, after

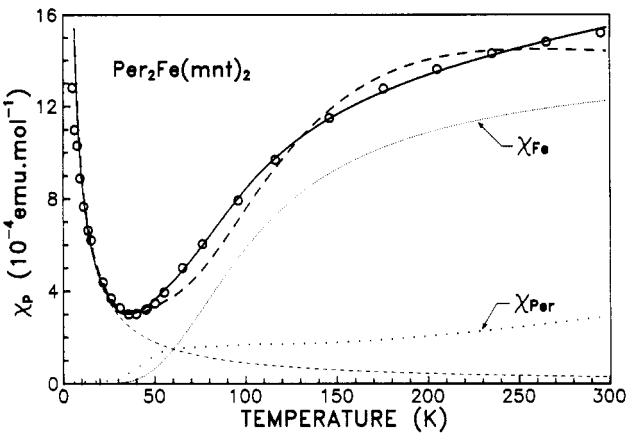

Figure 8. Paramagnetic susceptibility of $(Per)_2Fe(mnt)_2$ as a function of temperature T (from experimental values by considering a diamagnetic contribution of 4.2×10^{-4} emu/mol). The solid line represents the fit of the eqs 2 and 3; Curie tail (dashed line); $Fe(mnt)_2^-$ contribution, χ_{Fe}, given by eq 2 (lower thin line); conduction perylene electrons contribution, χ_{Per} (dotted line). The dashed line through the points represents the best fit using eqs 1 and 3 (see text).

correction for a diamagnetic contribution estimated from tabulated Pascal constants as 4.2×10^{-4} emu/mol, is shown in Figure 7. At room temperature, χ_P is 3.2×10^{-4} emu/mol with a slight decrease upon cooling until 80 K, where the susceptibility reaches 2.3×10^{-4} emu/mol. At 73 K, the temperature of the metal to insulator transition, a sharp decrease in susceptibility is observed that in the range 10–60 K becomes temperature independent with a value of 0.7×10^{-4} emu/mol. This value most probably reflects the error in the estimate of the diamagnetic contribution.

Typical paramagnetic molar susceptibility, χ_P, results obtained from magnetization measurements on a freshly prepared $Per_2Fe(mnt)_2$ sample, after correction for a diamagnetic contribution estimated from tabulated Pascal constants as 4.2×10^{-4} emu/mol, are shown in Figure 8. At low temperatures the results are dominated by a relatively large Curie tail, ascribed to impurities and defects, that was found sample dependent and increasing with time, denoting sample aging in the time scale of several weeks and reaching values of twice that of freshly prepared sample. Above 250 K the molar paramagnetic susceptibility is $\simeq 15 \times 10^{-4}$ emu/mol (1.9×10^{-8} SI units) a value rather larger than that of the Co analogue, denoting the extra contribution of the spins in the $[Fe(mnt)_2]_2^{2-}$ units, in addition to a smaller Pauli-like contribution, χ_{Pauli}, due to the conduction electrons in the perylene chains. The Pauli contribution is expected to be identical to the observed χ_P in $(Per)_2Co(mnt)_2$ with an adjustment for the smaller T_{M-I}. The contribution of the $Fe(mnt)_2^-$ units, χ_{Fe}, is expected to result from the antiferromagnetic interaction of the $Fe(mnt)_2^-$ spins in dimers with an energy J and with negligible interdimer coupling. This contribution depends on the total spin S in each $Fe(mnt)_2^-$ unit, which has previously been argued, without definitive proof, to be either $S = {}^1/_2$[12] or $S = {}^3/_2$.[29] In the case of $S = {}^1/_2$, this results in a singlet–triplet susceptibility per mole of $Fe(mnt)_2^-$ given by[30]

$$\chi_{Fe1/2} = (Ng^2\mu_B^2/k_BT)[\exp(-2J/k_BT) + 3]^{-1} \qquad (1)$$

where g is the Landē constant, μ_B the Bohr magneton, and N Avogadro's number. Alternatively, in the case of $S = {}^3/_2$, assuming as before an isotropic exchange J and neglecting a small biquadratic term, we have a contribution of the type[30]

$$\chi_{Fe_{3/2}} = \frac{Ng^2\mu_B^2}{k_BT}((\exp(2J/k_BT) + 5\exp(6J/k_BT) + 14\exp(12J/k_BT))/(1 + 3\exp(2J/k_BT) + 5\exp(6J/k_BT) + 7\exp(12J/k_BT))) \qquad (2)$$

(29) Gray, H. B.; Billig, E. *J. Am. Chem. Soc.* **1963**, *85*, 2019.
(30) Carlin, R. L.; *Magnetochemistry*; Springer-Verlag: Berlin, 1986.

Table V. Properties of Different α Phases of $(Per)_2[M(mnt)_2]$[a]

M	n	S	σ_{RT}, Ω^{-1} cm^{-1}	S_{RT}, μV/K	T_{M-I}, K	T_ρ, K	2Δ, meV	ref
Au	8	0	700	32	12	16	3.5	3, 41
Cu	8	0	700	38	32	40	20	6
Pt	7	$^1/_2$	700	32	8	18	8.6	1, 3, 41
Pd	7	$^1/_2$	300	32	28	80		2, 3
Ni	7	$^1/_2$	700	35	25	50	15	6
Co	6	0	200	42	73	95	60	*b*
Fe	5	$^3/_2$	200	42	58	105	50	*b*

[a] n, number of d electrons; S, spin; T_{M-I}, metal insulator transition temperature; T_ρ, minimum electrical resistivity temperature; 2Δ, low-temperature gap derived by resistivity. [b] This work.

Therefore, the results of paramagnetic susceptibility of $(Per)_2Fe(mnt)_2$, χ_P, were tentatively fitted by the sum of the contributions given by expression 3, using for χ_{Fe} either eq 1 or

$$\chi_P = (C/T) + \chi_{Pauli} + \chi_{Fe} \quad (3)$$

2 and for χ_{Pauli} data of the Co compound with rescaled temperatures to account for the difference in the transition temperatures (see Figure 8). Although some previous studies suggested that $Fe(mnt)_2^-$ could have $S = ^1/_2$, a significantly better fitting was obtained by considering expression 2 for $S = ^3/_2$, as shown by the solid line in Figure 8. The best fit with expressions 2 and 3 was obtained, in reasonable agreement with the experimental results, with $C = 89 \times 10^{-4}$ K emu/mol, corresponding to a Curie tail due to 2.4% of $S = ^1/_2$ spins (or 0.5% of $S = ^3/_2$ spins) (dashed line) and $\chi_{Fe3/2}$ given by eq 2 with $C' = (Ng^2\mu_B^2)/(k_BT) = 1.342$ K emu/mol (corresponding to $g \simeq 1.85$) and $-2J/k_B = 300$ K (lower solid line). In contrast to this, a much poorer fit was obtained with eqs 1 and 3 (dashed line through the points in Figure 8). This predicts a clear maximum of χ characteristic of the singlet–triplet law absent in the experimental results that increase from $\simeq$40 K to room temperature and gives a much larger value of $C' = 2.156$ K emu/mol, implying very large values of $g \simeq 3.0$.

A similar good fit considering pairs of $S = ^3/_2$ spins is also observed in the strongly dimerized compounds $[(C_2H_5)_4N]_2[Fe(mnt)_2]_2$ and $[(n\text{-}C_4H_9)_4N]_2[Fe(mnt)_2]_2$ whose susceptibilities, for the sake of comparison, were also measured in the present work. Their paramagnetic contributions are displayed in Figure 9, after correction for diamagnetic contributions estimated as 2.37×10^{-4} and 3.30×10^{-4} emu/mol, respectively. It is remarkable that for these compounds a large Curie tail persisted after multiple recrystallizations. The best fit to the experimental data of these compounds using eq 2 and 3, but here obviously without considering the Pauli term (continuous line in Figure 9), was obtained with $C = 227 \times 10^{-4}$ and 310×10^{-4} K emu/mol, $-2J/k_B = 374$ and 394 K, and $C' = 1.661$ and 1.579 K emu/mol for the ethyl and butyl compounds, respectively. It should be noted that, without showing detailed temperature-dependent susceptibility results, the deviation to the simple singlet–triplet model was already noticed[12] for $[(C_2H_5)_4N]_2[Fe(mnt)_2]_2$. The present results clearly show that $Fe(mnt)_2^-$ in these compounds is in a high-spin configuration of $S = ^3/_2$ as found in other square pyramidal complexes of iron such as the halobis(dithiocarbamates), e.g., $Fe[S_2CN(C_2H_5)_2]_2Cl$.[31,32]

Discussion

The average structure of $(Per)_2Fe(mnt)_2$ is similar to that of the other metallic compounds (α phases) of these family with M = Pt, Pd, Au, Ni, and Cu. The main structural difference with the M = Fe and Co compounds is the doubling of the unit cell along *b*. Synchroton radiation data on the Fe compound also shows a cell doubling along *c*. This is ascribed essentially to the dimeric nature of the $M(mnt)_2$ units, as shown in case of the Fe compound by Mössbauer spectra, which further indicates that no major changes in the Fe coordination occur at the phase transition. This is also supported by the similarity of the estimated contribution of the $Fe(mnt)_2$ units to the magnetic susceptibility of $(Per)_2Fe(mnt)_2$ with those of $[(C_2H_5)_4N]_2[Fe(mnt)_2]_2$ and $[(n\text{-}C_4H_9)_4N]_2[Fe(mnt)_2]_2$, also strongly suggesting the same dimeric structure in all these compounds. It should also be noted that to the best of our knowledge there are no known examples of reported structures of bis(dithiolene) complexes of Fe(III) which are not dimeric. In the case of Co, dimeric structures are also well-known for $(n\text{-}C_4H_9)_4NCo(C_6Cl_4S_2)_2$[33] or $Co[S_2C_2(CF_3)_2]_2$.[34] At the present we cannot completely exclude the possibility of a distortion also in the perylene chains. A similar situation is expected in the analogue with M = Co that, in view of the closely related crystalline parameters and physical properties, can have an isomorphous structure.

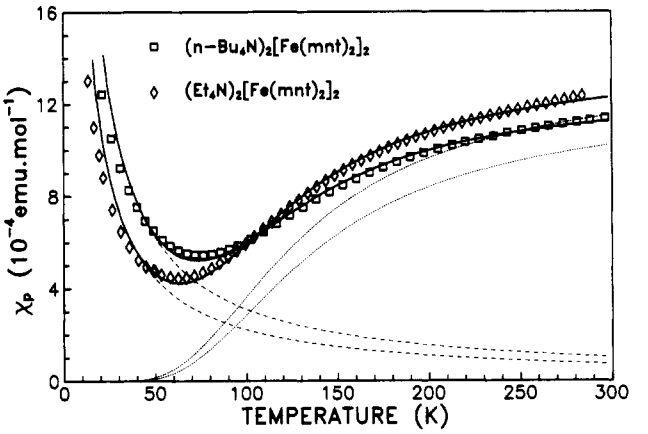

Figure 9. Paramagnetic susceptibility of $[(C_2H_5)_4N]_2[Fe(mnt)_2]_2$ (diamonds) and $[(n\text{-}C_4H_9)_4N]_2[Fe(mnt)_2]_2$ (squares) as a function of temperature T. The solid lines represent the fit to a sum of Curie tail (dashed lines) with eq 2 (lower thin lines) (see text).

In spite of the lattice doubling along *b*, and as shown in Table V, at high temperatures the transport properties of both compounds with M = Fe and Co are similar to the other metallic members (α phases) of this family with M = Pt, Pd, Au, Ni, and Cu.[1-3,6] The main difference is the higher metal to insulator transition temperature and a slightly smaller electrical conductivity. The nature of these phase transitions will be discussed at the end of this section. In many crystals measured ($\simeq$20 for each metal) from different batches, evidence was never found for the occurrence of the semiconducting β-phases, which have been detected for M = Cu,[6] Ni,[6] and Au.[35]

Thermopower measurements in the other metallic members of this series (M = Pt, Pd, Au, Ni, and Cu)[3,6] gave results above their metal–insulator transition temperature with a temperature dependence identical to those found for M = Fe and Co, with slightly smaller values. These results have been interpreted as an indication of electrical transport in a $^3/_4$-filled band of perylene chains with bandwidths estimated as 0.6 eV.[3] In the case of the present compounds, the dimerization of the lattice along *b* opens a gap and makes the $^3/_4$-filled bands of the regular chains became effectively $^1/_2$ filled. A $^1/_2$-filled band, being symmetrical around the Fermi level, would give an almost zero thermopower. The large thermopower observed in the Fe and Co compounds suggests

(31) Martin, R. L.; White, A. H. *Inorg. Chem.* **1967**, *6*, 712.
(32) Hoskins, B. F.; Martin, R. L.; White, A. H. *Nature* **1966**, *211*, 627.
(33) Backer-Hawkes, M. J.; Zui Dori; Heisenberg, R.; Gray, H. B. *J. Am. Chem. Soc.* **1968**, *90*, 4253.
(34) Henemark, J. H.; Lipscomb, W. H. *Inorg. Chem.* **1965**, *4*, 1729.
(35) Gama, V. P., unpublished.

that, as in case of the $(TMTSF)_2X$ family,[36] the dimerization potential in the perylene conducting chains is very small, inducing a small gap that does not change significantly the band structure at the Fermi level. The slightly larger thermopower in these cases (42 μV/K when compared with 32 μV/K in M = Au, Pt, and Pd compounds[3]) should reflect essentially a decrease of the bandwidth as a consequence of the slightly larger perylene intermolecular distances (3.36 (3) Å for Fe compared to 3.32 (1) Å for M = Pt, Au, and Pd) with the same overlap mode.

EPR measurements in the Co compound at room temperature showed only a single narrow (LW = 3.2 G at room temperature, decreasing to 1 G at 250 K) and nearly isotropic line ($2.0038 < g < 2.0043$)[37] whose temperature-dependent intensity closely follows the observed temperature dependence of static magnetic susceptibility reported in this work. These results are compatible with an EPR signal and static magnetic susceptibility both due only to the conducting perylene chains, giving a Pauli-like contribution with the $Co(mnt)_2^-$ units being diamagnetic. The observed small decrease in the susceptibility of the perylene chains in $Per_2Co(mnt)_2$ upon cooling from room temperature to 100 K has been also observed in other low-dimensional molecular metals like TTF-TCNQ[38] or $TMTSF_2X$ salts.[39,40] The tight binding model for uncorrelated electrons predicts a Pauli contribution given by expression 4,[41,42] where t is the transfer integral between su-

$$\chi_{Pauli} = N\mu_B^2/[t\pi \sin(\pi\rho/2)] \quad (4)$$

cessive perylene molecules and ρ is the number of electrons per perylene molecule. From the room temperature susceptibility $\chi_P = 3.2 \times 10^{-4}$ emu/mol and considering $\rho = {}^3/_2$, a bandwidth 4t of $\simeq$0.2 eV is obtained, a value much smaller than 0.5 eV obtained from thermopower. This discrepancy, which would not be removed even with a possible overestimation of χ_P due to an error of 0.7×10^{-4} emu/mol in the diamagnetic contribution, is taken as an indication of enhancement of the paramagnetic susceptibility by the electron correlations as in other molecular metals.[38-40]

The static susceptibility of $Per_2Fe(mnt)_2$ has a temperature dependence very different from the integrated intensity of the EPR line previously reported.[37] This line is much broader (LW = 32 G) than in the Co compound, but also nearly isotropic ($2.0037 < g < 2.0042$) line.[37] This large line width is comparable with those observed in the analogues with paramagnetic $M(mnt)_2^-$ units like M = Pt[43] and Ni,[37] but in the present study, as opposed to the above cited cases, the g values are close to those of the perylene cation and therefore do not denote exchange interactions between the perylene electrons and the spins in the $Fe(mnt)_2^-$ units. Therefore it can be concluded that the integrated intensity of the EPR line contains essentially the contribution of the perylene chains and the static magnetic susceptibility measurements show that the susceptibility in this compound is dominated by the unpaired electrons in the strongly dimerized $Fe(mnt)_2^-$ units with $S = {}^3/_2$, and without significant anomalies at T_{M-I}.

In the compounds with M = Pt and Pd, it was shown that the metal to insulator transition is associated with one-dimensional instabilities that lead to the dimerization of the lattice along b and a magnetic susceptibility decrease at T_{M-I}.[2] These structural effects were not seen in the M = Au compound, where the $Au(mnt)_2^-$ unit is diamagnetic and whose respective perylene compound in earlier studies did not show a clear metal–insulator transition.[2] Therefore it was suggested that, in the cases with magnetic $M(mnt)_2^-$ chains (M = Pt and Pd), the metal to insulator transition should result from the instability of the one-dimensional conducting electrons of the perylene chains coupled to the instability of the $M(mnt)_2^-$ magnetic chains of the spin-Peierls type.[2,4] The dimerization of the $M(mnt)_2^-$ units, driven by the magnetic interaction, would in this case lead to an insulator state in the perylene chains due to sizable Coulombic repulsions of the electrons. More recently it was shown that a M–I transition occurs also in the Au compound at 12 K,[44] and the temperature dependence of the ^{1}H-NMR relaxation rate in M = Au and Pt compounds provided evidence for relatively small electronic Coulombic repulsions.[45]

The fact that, as shown in the present study, compounds with M = Fe and Co, already having a dimerization of the $M(mnt)_2$ units at room temperature, are metallic and that, independently of the magnetic (M = Fe) or diamagnetic nature (M = Co) of the $M(mnt)_2^-$ species, they undergo a metal to insulator transition at low temperatures shows that Coulombic correlations are relatively unimportant in these compounds and suggests that the M–I transition occurs at least in the M = Co and Fe compounds, by the $2k_F$ (tetramerization) transition of the perylene chains. A more clear description of the nature of the transition in this case waits for more detailed EPR and X-ray diffuse scattering studies under way.

Acknowledgment. We acknowledge L. Alcâcer for continuous encouragement, C. Bourbonnais for fruitful discussions, and J. P. Pouget and S. Ravy for help in X-ray photographic experiments. This work was partially supported by EEC under ESPRIT Basic Research Action 3121 and by Junta Nacional de Investigação Científica e Tecnológica under contracts 798/90/MPF and PMCT/C/CEN/367/90. The stay of G.B. at LNETI was supported by CNRS.

Registry No. I, 198-55-0; $(Per)_2[Fe(mnt)_2]$, 136086-81-2; $(Per)_2[Co(mnt)_2]$, 136020-67-2; $(Per)_2Co(mnt)_2]CH_2Cl_2)_{0.5}$, 139039-75-1; $[(n\text{-}C_4H_9)_4N]_2[Fe(mnt)_2]$, 31358-28-8; $[(n\text{-}C_4H_9)_4N]_2Co(mnt)_2]$, 18958-58-2; CH_2Cl_2, 75-09-2.

Supplementary Material Available: Tables listing atomic displacement parameters and selected bond distances and angles (3 pages); tables of observed and calculated structure factors (6 pages). Ordering information is given on any current masthead page.

(36) Bechgaard, K.; Jacobsen, C. S.; Mortensen, K.; Pedersen, H. J.; Thorup, N. *Solid State Commun.* **1980**, *33*, 1119.
(37) Gama, V. P.; Henriques, R. T.; Almeida, M.; Alcâcer, L. *Synth. Met.* **1991**, *42*, 2553.
(38) Scott, J. C.; Garito, A. F.; Heeger, A. J. *Phys. Rev. B* **1974**, *10*, 3131.
(39) Jacobsen, C. S.; Pedersen, H. J.; Mortensen, K.; Rindorf, G.; Thorup, N.; Torrance, J. B.; Bechgaard, K. *J. Phys. C: Solid State Phys.* **1982**, *15*, 2651.
(40) Scott, J. C.; Pedersen, H. J.; Bechgaard, K. *Phys. Rev. Lett.* **1980**, *45*, 2125.
(41) Shiba, H. *Phys. Rev. B* **1972**, *6*, 930.
(42) Torrance, J. B.; Tomkiewicz, Y.; Silverman, B. D. *Phys. Rev. B* **1977**, *15*, 4738.
(43) Henriques, R. T.; Alcâcer, L.; Almeida, M.; Tomic, S. *Mol. Cryst. Liq. Cryst.* **1985**, *120*, 237.
(44) Bonfait, G.; Lopes, E. B.; Matos, M. J.; Henriques, R. T.; Almeida, M., *Solid State Commun.* **1991**, *80*, 391.
(45) Bourbonnais, C.; Henriques, R. T.; Wzietek, P.; Köngeter, D.; Voiron, J.; Jerome, D. *Phys. Rev. B* **1991**, *44*, 641.